 FDMP, vol.7, no.3, pp.279-301, 2011

Binary Collisions of Immiscible Liquid Drops for Liquid Encapsulation

Carole Planchette[1], Elise Lorenceau[1] and Günter Brenn[2]

Abstract: This work is dedicated to a general description of collisions between two drops of immiscible liquids. Our approach is mainly experimental and allows us to describe the outcomes of such collisions according to a set of relevant parameters. Varying the relative velocity U as well as the impact parameter X we can build for each pair of investigated liquids a nomogram X,U showing three possible regimes: coalescence, head-on separation and off-center separation. In this paper, we also study the influence of the liquid properties, i.e. viscosity, density, surface and interfacial tensions using a set of aqueous glycerol solutions together with a set of silicon and perfluorinated oils. We show that the coalescence regime always leads to full spreading of the oil on the aqueous drop (encapsulation) in contrast to the separation regimes where part of the oil is expelled from the encapsulated drop. For head-on separation, three different mechanisms were identified: reflexive separation, single-reflex separation, and crossing separation. Concerning the stability limits of such collisions, the aqueous phase seems to be of little influence in the range of studied liquids. For off-center collisions, the efficiency of the encapsulation is measured via the amount of oil forming the encapsulating shell. We show that the thickness of this coating can be tuned independently from the liquid properties and drop relative velocity by varying the impact parameter. Finally, we briefly address the case of unequal sized drops and the regimes observed for head-on separation.

Keywords: Binary drop collisions, immiscible liquids, crossing separation, instability onset, encapsulation efficiency.

[1] Laboratoire de Physique des Matériaux Divisés et des Interfaces, FRE 3300 CNRS, Université Paris-Est, 5 boulevard Descartes, 77454 Marne-la-Vallée cedex 2, France

[2] Institute of Fluid Mechanics and Heat Transfer, Graz University of Technology, Inffeldgasse 25/F, 8010 Graz, Austria

1 Introduction

For already several decades, drop collisions have been of high interest for understanding natural phenomena as well as for improving technical processes. Meteorology and, more precisely, the investigation of rainfall conditions have triggered part of the work, see Brazier-Smith, Jennings, and Latham (1972). Spray studies, which are essential for applications such as spray combustion or spray drying, have also contributed to the development of this research field especially with the focus of the possible collision outcomes with, for instance Ashgriz and Poo (1990), Jiang, Umemura, and Law (1992), Qian and Law (1997), Orme (1997), Brenn, Valkovska, and Danov (2001), Gotaas, Havelka, Jakobsen, Svendsen, Hase, Roth, and Weigand (2007). More recently, the case of collisions between drops consisting of different, in part immiscible, liquids has gained some interest. We can cite Gao, Chen, Pu, and Lin (2005), Chen and Chen (2006), Chen (2007), and Planchette, Lorenceau, and Brenn (2010). Indeed, such collisions occur in combustion engines, but can also be generated in case of a nuclear reactor accident to collect and neutralize dangerous droplets, or can be used as a process for the encapsulation of liquids in the food sciences and in pharmacology. This last example, which is of great importance for drug delivery, appears as a very promising application of our current work.

To fully describe binary collisions of drops of the same liquid, the following parameters are needed: the ambient air properties, the liquid properties density ρ, surface tension σ, and viscosity μ, together with the drop diameters D_1, D_2 and relative velocity U, plus a geometrical factor called the impact parameter x, which measures the eccentricity of the impact. An illustrating sketch is given in Fig. 1.

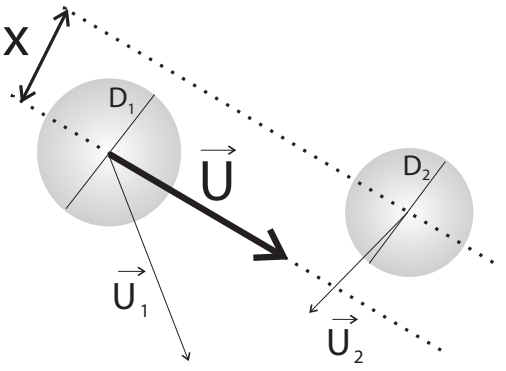

Figure 1: Binary collision of drops. Definition of relative velocity U and impact parameter x.

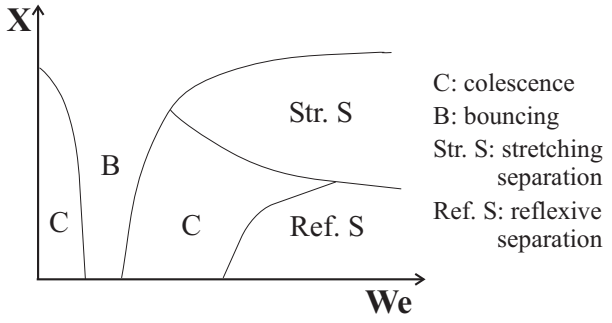

Figure 2: Typical (X, We) nomogram obtained for binary collisions of equal-sized drops. A similar scheme can be found in Qian and Law (1997).

If we neglect variations of the gaseous ambient medium, these parameters can be put in a dimensionless form with the following numbers: the diameter ratio of the drops $\Delta = D_1/D_2$, the dimensionless impact parameter $X = 2x/(D_1 + D_2)$, and the Weber and Ohnesorge numbers defined as $We = U^2 D_1 \rho/\sigma$ and $Oh = \mu/\sqrt{\sigma D_1 \rho}$, respectively. Considering equal sized drops with a given Ohnesorge number, the binary collision outcome can be represented by an (X, We) nomogram, as sketched in Fig. 2. The different regimes that appear are characterized by different outcomes of the collision: coalescence (C) leads to complete merging of the colliding droplets; bouncing (B) is characterized by a rebound of the drops, where no mass is exchanged between the drops; reflexive separation (Ref. S) occurs at sufficiently high Weber number of the collision with moderate impact parameter and leads to breakup of the collided drops, leaving most of the liquid mass of each droplet on the side from where it has arrived; stretching separation (Str. S) occurs in grazing collisions and also leads to the formation of several smaller droplets, involving a cross-over of liquid mass together with the break-up of a liquid filament formed between the main masses of the colliding drops. These regimes are known from experiments with different, miscible liquids also (Gao, Chen, Pu, and Lin (2005), Chen (2007)), where the differences in the liquids just slightly move the regime boundaries with respect to those for drops of the same liquid. Only the bouncing regime is not reported for ethanol and water drop collisions by Gao, Chen, Pu, and Lin (2005). For different, immiscible liquid drop collisions, the above described regimes also occur, but with some detail differences in the mechanisms involving separation (Chen and Chen (2006)). Also, Planchette, Lorenceau, and Brenn (2010) discovered a new mechanism of separation caused by the differences in the immiscible liquid properties. The regimes for the different, immiscible liquids are one subject of the present work.

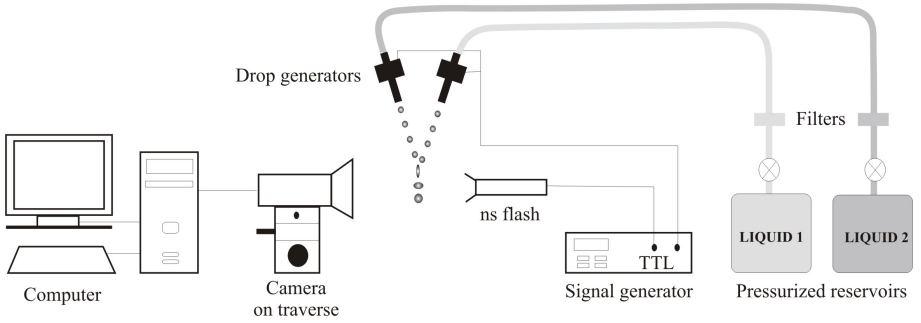

Figure 3: Experimental set-up consisting of two droplet generators connected to two immiscible liquid reservoirs. The generator positions can be adjusted with micro-control traverses. The ultra-fast flash allows illumination of the collisions, which are recorded by the camera.

In this paper we develop similar nomograms for binary collisions of immiscible liquid drops. Our experimental work is focused on the survey of the outcomes and their mechanisms, together with the modifications of the stability limits by the liquid properties. A very promising and reliable application of this study is shown with the control of the shell thickness enabling a tunable encapsulation of one droplet. Finally, collisions between unequal-sized drops are studied.

2 Experimental facility

2.1 Droplet generators and image processing

To achieve binary collisions of immiscible liquid drops in a controlled way, we use two droplet generators by Brenn, Tropea, and Durst (1996). The drop generators consist of a tube with a nozzle of different possible sizes, producing a laminar jet. An integrated piezo-ceramic, excited by an electrical signal at a given frequency, creates a disturbance of the jet and leads to its break-up with a given wave length (Rayleigh-type breakup). As a result we obtain continuous streams of monodisperse drops of variable size and defined trajectories. Those trajectories are adjusted via the displacement of the generators on micro-control traverses. The accuracy of $\pm 2\mu$m and $\pm 2^\circ$ allows us to vary accurately their relative impact velocity U, as well as the non-dimensional impact parameter X. The set-up is shown in Fig. 3. An ultra-fast flash in the order of 10ns illuminates the region of impact, and a PCO Sensicam video camera produces movies of the collisions. By aliasing the generator frequency with the flash frequency, we can record the same collision at different phases. Pictures are then extracted from the movies in order to determine the sizes

of the drops before and after the collision, deduce the relative drop velocity U, and calculate the normalized impact parameter X. In the first part of our study, the drop sizes varied between 180 μm and 210 μm, and the size ratio Δ of the two colliding drops equals unity, except for the final part of the study on collisions of unequal-sized drops.

2.2 Immiscible liquids

In our experiments we use pairs of immiscible liquids consisting of one aqueous phase and one oil phase. The pairs of liquids were selected according to their surface and interfacial tensions with the aim to enable a complete encapsulation of the aqueous phase by the oil phase. As the aqueous phase, mixtures of glycerol with water were chosen (G), where the dynamic viscosity may be varied by the composition of the mixtures, while the surface tension against air, as well as the density, remain fairly constant. The glycerol concentrations are given in weight percent with the following range: from 20% to 55%, which correponds to a viscosity range of 1.76 mPa·s to 7.90 mPa·s. As the oil phase, we use four different types of silicon oil (SO) plus two mixtures of them. This set of oils allows us to investigate the influence of the dynamic viscosity, keeping the density and surface tension almost unchanged. Additionally, we also used the fluorinated oil perfluorodecaline (perfluo) which has similar properties as the silicon oils, except for its density. Table 1 puts together the physical data of the liquids relevant for the collisional interaction. From those thermodynamic data we can calculate a spreading parameter $S = |\sigma_w - \sigma_o| - \sigma_{ow}$. Since $S \geq 0$, the oils are going to spread on the aqueous phase until full encapsulation is achieved.

3 Results and discussion

3.1 Survey of regimes and mechanisms

In order to validate our experimental set-up, we first realized binary collisions of drops of a glycerol solution at 40%. For such collisions of drops of the same liquid, the four expected regimes could be observed: bouncing, permanent coalescence, reflexive separation for head-on collisions, and stretching separation for the off-center cases. Replacing one of the two glycerol drops by the silicon oil M3, we observed very similar outcomes: permanent coalescence plus two separation regimes for head-on and off-center collisions. Note that the bouncing regime has not been observed within our range of impact velocities, but its occurrence has been proven by Chen and Chen (2006). To keep the comparison with different liquid pairs as clear as possible, we replaced the (X, We) nomogram used for drops of the same liquid by (X,U) nomograms. As shown in Fig. 4, the nomogram obtained for

Table 1: Physical data of the investigated liquids at 20°C. (*) Values from data sheet of dealer Carl Roth; interfacial tensions against (1) SO M3; (2) SO M5; (3) G 50%.

Liquid	Density kg/m^3	Dynamic viscosity mPa·s	Surface tension mN/m	Interf. tension mN/m
G 20%	1047.9	1.76	70.7	37.7[1]
G 30%	1072.9	2.50	70.3	36.7[1]
G 40%	1098.8	3.72	69.5	34.9[1]
G 50%	1126.0	6.00	68.6	34.8[1]
G 50%	1126.0	6.00	68.6	34.3[2]
G 55%	1139.0	7.90	68.1	33.8[1]
SO M3	892.2	2.79*	19.5*	34.9[3]
SO M5	913.4	4.57	19.5	-
SO M5 + 10	925.3	6.6	19.8	-
SO M10	937.2	9.37*	20.1	-
SO M10 + 20	944.5	14.28	20.3	-
SO M20	951.8	19.0*	20.7	-
PERFLUO	1934.9	5.5*	17.8	36.5[3]

immiscible liquids looks very similar to the one for drops of the same liquid. Despite such similarities, it is important to note that the mechanisms leading to the separation of the drops are completely different with immiscible liquids.

Coalescence occurs for relatively low impact parameters and velocities. Typically $X \leq 0.3$ and $U \leq 2\ m/s$. The two drops come into contact, get strongly distorted, and lead to an encapsulated drop (aqueous core with an oil shell), which slowly relaxes to a spherical shape due to surface tension and viscous losses during the relaxation from the distorted state. A picture of such a collision is given in Fig. 5.

Off-center separation takes place when increasing the impact parameter independently from the relative velocity ($X \geq 0.6$). The oil which starts to spread on the aqueous phase forms a filament between the two drops. Because of their opposite trajectories, the drops stretch this liquid bridge, leading to its pinch-off and breakup. In contrast to binary collisions of drops of the same liquid, the complex formed after impact is not symmetric. This observation was expected, since the two liquids do not play a symmetric role any more, see Fig. 6.

The most complex case is seen with head-on separation. For binary collisions of drops of the same liquid, the so-called reflexive separation occurs. The drops are first compressed together. The disc-like complex relaxes under the excess of surface

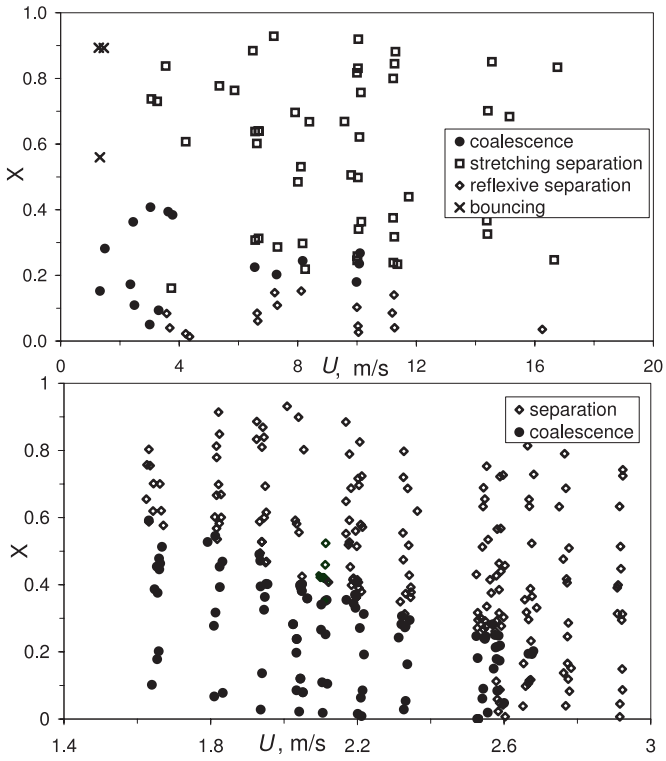

Figure 4: Top: (X,U) nomogram obtained for binary collisions of two drops of G40%. Bottom: (X,U) nomogram obtained for binary collisions of a drop of G40% with a drop of SO M3. In both cases, the drop diameter is 200μm $\pm$ 10%. Considering the respective range of investigated velocities, the nomograms present important similarities.

energy and the internal flows. A cylinder is generated, which stretches and breaks up, leading to two main drops (at the ends of the cylinder) plus eventually some additional satellites (from the central part of the cylinder). The name of this process comes from the fact that the liquid of the drop coming from, e.g., the right side before impact is mainly found on the right drop born by the separation. The impact plane acts as a mirror and redistributes the liquid equally on both sides.

For immiscible liquids, in the range of our combinations of liquids, different mechanisms have been seen. The full description of those processes and their domains of occurrence are still under investigation. In the limit of relatively small velocities (in the order of the threshold velocity U_0), and with our current knowledge, it

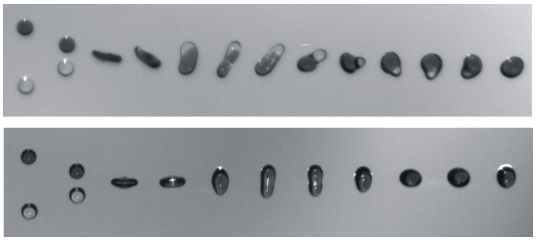

Figure 5: Top: a drop of glycerol at 50% encapsulated by a drop of SO M10, D=188μm, U=4.04m/s and X=0.22: Coalescence between a drop of glycerol at 50% and a drop of SO M20 , D=210μm, U=3.88m/s and X=0.00.

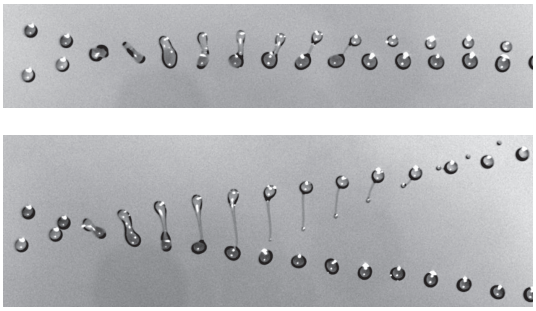

Figure 6: Stretching separation of a G 50% drop with a SO M10 drop. Top: D=204μm, U=4.00m/s and X=0.41. Bottom: D=206μm, U=3.99m/s and X=0.62. The dark drops consist of the dyed glycerol solution.

seems that when the liquid densities are of the same order, the viscosity ratio pilots the separation. If the encapsulating phase is not much more viscous than the encapsulated one, it can easily flow around it and find itself on the opposite side of the contact point. This excrescence gets stretched by the non dissipated kinetic energy and breaks up, leading to an aqueous drop fully encapsulated by an oil shell plus a second drop of pure oil coming from the excrescence break up. This mechanism termed *crossing separation* has first been described by us in Planchette, Lorenceau, and Brenn (2010) and can be seen in Fig 7. If the viscosity of the encapsulating phase becomes too high as compared to the encapsulated one, it will stretch the aqueous drop while flowing around. The resulting two-phase cylinder gets thinner and breaks. Two encapsulated drops are then generated. In the work of Chen and Chen (2006) this process is called single-reflex separation. One drop mainly consists of the aqueous phase (and would correspond to the encapsulated drop of a crossing separation), while the other one contains much more oil (and would corre-

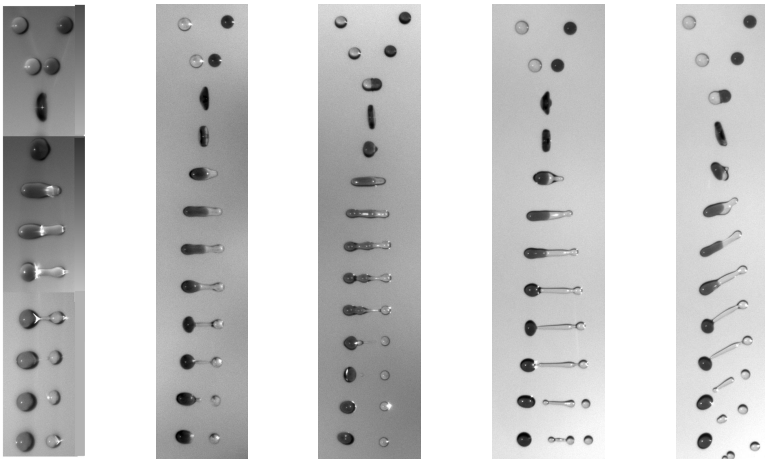

Figure 7: Some examples of crossing separations. The dark droplets are the aqueous phase, the oil remains transparent. From left to right: Glycerol at 50% (G 50%) and SO M3, D=182μm, U=2.77m/s and X=0.04. G 50% with SO M5, D=211μm, U=3.97m/s and X=0.05. G 50% with SO M5, D=207μm, U=4.84m/s and X=0.01. G 50% and SO M3, D=204μm, U=3.82m/s and X=0.05. Finally G 50% and SO M3, D=202μm, U=3.79m/s and X=0.17.

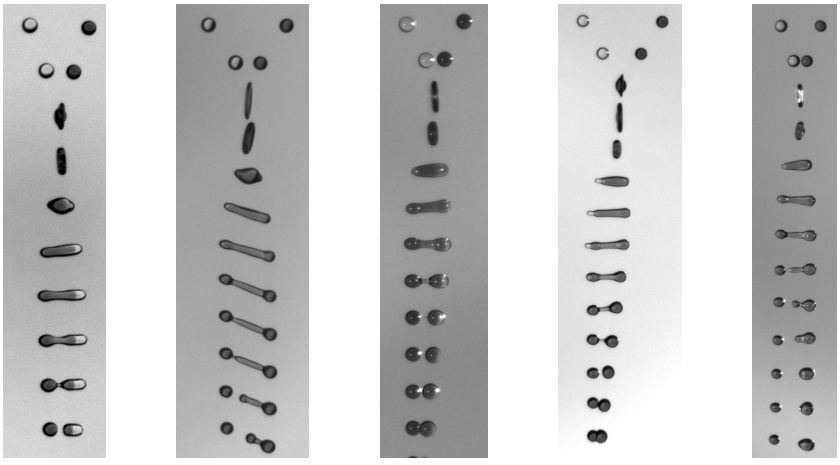

Figure 8: Head-on separations leading to two encapsulated drops and so-called single-reflex separation. Dark droplets consist of glycerol solutions, the transparent ones are oil. From left to right: Glycerol at 50% and mixture of SO M5 / SO M10 at 1:1. D=192μm, U=3.90m/s and X=0.00. Glycerol at 50% with SO M20, D=206μm, U=7.38m/s and X=0.04. Glycerol at 50% and SO M10, D=188μm, U=4.78m/s and X=0.01. Glycerol at 60% with SO M10, D=198μm, U=6.72m/s and X=0.01. Glycerol at 20% and SO M10, D=200μm, U=4.32m/s and X=0.02.

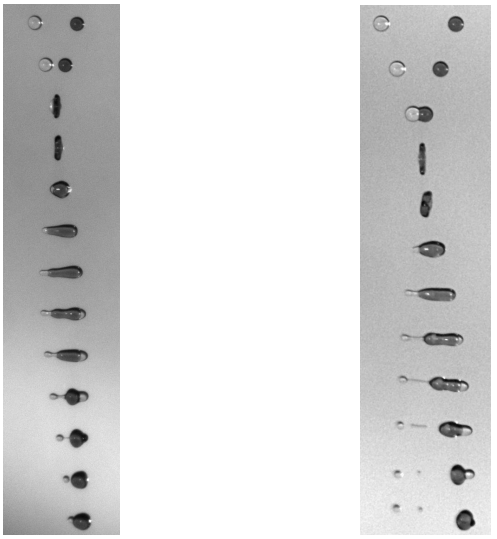

Figure 9: Reflexive separation between a G 50% drop (right upstream) with a perfluorodecaline drop. Left: D=198μm, U=3.16m/s and X=0.02; right: D=202μm, U=3.95m/s and X=0.03.

spond to the expelled oil of a crossing separation). In our work, we cannot always identify a pure oil drop in the separated drops. Moreover, the smaller drop is found where we used to find the encapsulated drop of a crossing separation, and therefore the same kind of liquid distribution must result, see Fig. 8 and pictures in Chen and Chen (2006).

Finally, if the liquid densities are not of the same order, the distribution of the encapsulated phase is changed: part of it stays on the contact side, while the rest flows to the opposite side. The bigger excrescence breaks up under the effect of surface tension. This can happen on the impact side, creating a reflexive separation where a pure oil droplet can be identified, see Fig. 9.

The occurrence of these three mechanisms of head-on separation is given in Table 2 for our current experimental combinations with equal-sized drops.

3.2 Influence of the encapsulated liquid viscosity in the crossing separation domain

In this part of the paper we estimate the influence of the encapsulated liquid viscosity on the stability limits of the collisions. For this purpose we used only the Silicon Oil M3 as the oil phase and varied the viscosity of the glycerol solution. For each glycerol concentration we obtain an (X,U) nomogram where both coales-

Table 2: Occurrence of the different mechanisms of head-on separation for the investigated pairs of liquids. Drop diameters are 200μm $\pm 20\%$.

Oil phase	Aqueous phase	Head-on separation mechanism
SO M3	Glycerol 20%, 30%, 40%, 50%, 55%	Crossing separation
SO M5	Glycerol 40%	Single-reflex sep.
SO M5	Glycerol 50%	Crossing separation
SO M5 + M10	Glycerol 50%	Single-reflex sep.
SO M10	Glycerol 20%, 30%, 40%, 50%, 60%	Single-reflex sep.
SO M10 + M20	Glycerol 50%	Single-reflex sep.
SO M20	Glycerol 50%	Single-reflex sep.
PERFLUO	Glycerol 50%	Reflexive separation

Table 3: Ranges of critical values of ζ_p for different glycerol concentrations. The oil phase is SO M3.

Oil phase	Aqueous phase	Critical value of ζ_p
SO M3	Glycerol 20%	$2.9 < \zeta_p < 3.3$
SO M3	Glycerol 30%	$3.0 < \zeta_p < 3.3$
SO M3	Glycerol 40%	$2.8 < \zeta_p < 3.1$
SO M3	Glycerol 50%	$2.7 < \zeta_p < 3.0$
SO M3	Glycerol 55%	$2.7 < \zeta_p < 2.9$

cence and separation can be observed, see Fig. 10. It is important to note that, with these combinations of liquids, the mechanism of head-on separation is always the crossing separation.

These results clearly show that the influence of the encapsulated phase viscosity on the stability limits of the binary collisions is extremely low when staying in the crossing separation domain. This was to be expected. As the separation is due to break up of the oil phase excrescence, the aqueous phase is not directly involved, and its influence can be neglected. To predict the threshold velocity of the crossing separation U_0, we decided to measure the aspect ratio of the oil/glycerol complex $\zeta_p = b/a$ at a typical stage after the collision. See Fig. 11 for a definition of ζ_p.

We varied the glycerol concentration and noted the value of ζ_p at the stability limit. After a validation of this measurement by checking that, for a given collision, ζ_p remains almost constant with time, we built a modified Rayleigh criterion.

For SO M3, in the crossing separation domain, the stability limit is found for $2.7 \leq$

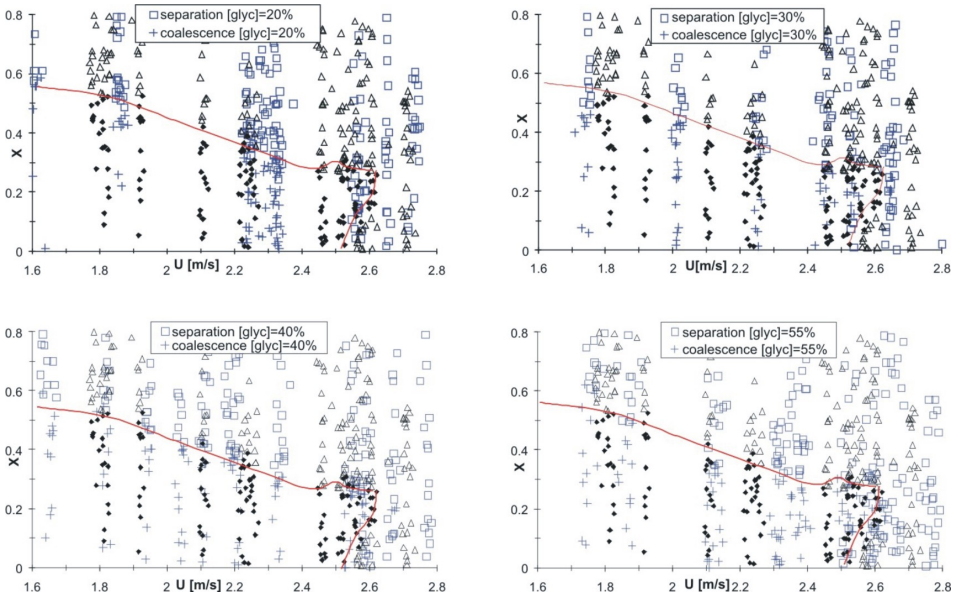

Figure 10: Nomograms of SO M3 / glycerol solution binary drop collisions. The black symbols in the four nomograms correspond to G 50% and allow for a direct comparison with the other concentrations.

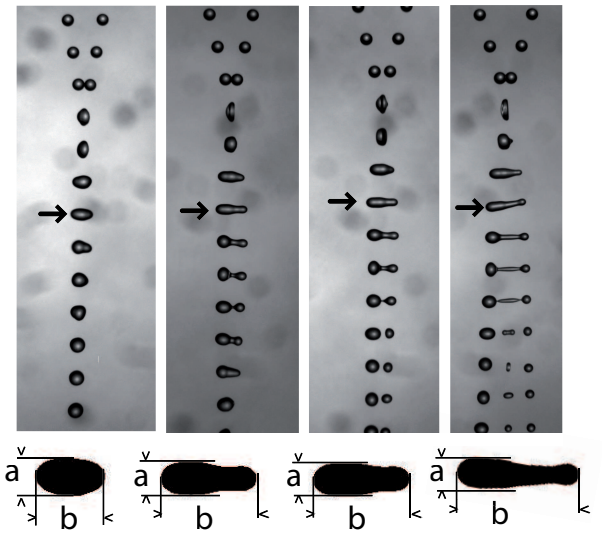

Figure 11: Collisions between G 50% and SO M3 drops. D≈200μm. From left to right U=1.81m/s, U=2.53m/s, U=2.60m/s, U=3.25m/s. The aspect ratio is defined as $\zeta_p = b/a$.

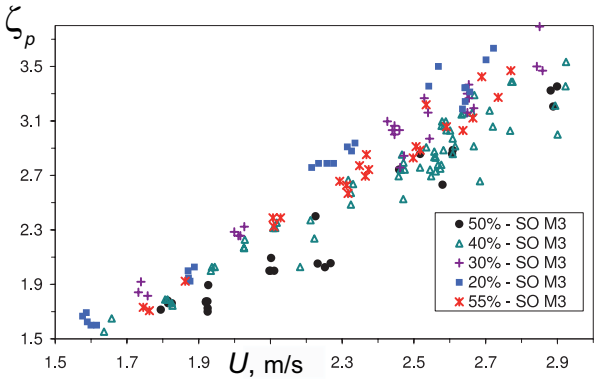

Figure 12: Evolution of ζ_p with U for different glycerol concentrations and velocities $>U_0$ and $<U_0$.

$\zeta_p \leq 3.2$, and this is not changed by varying the encapsulated liquid viscosity by a factor 4 (see Table 3 for details). This is our so-called modified Rayleigh criterion. Surprisingly, not only does the value of the critical ζ_p remain constant for various glycerol concentrations, but the behavior of this complex also remains similar: we observe a quasi linear growth of ζ_p with U, without any difference before and after the separation. See the results presented in Fig. 12. Nevertheless, the influence of the encapsulated liquid becomes important for the other mechanisms of head-on separation. At the present stage of our work, we do not have quantitative arguments to evaluate this influence and consequently this point is not discussed in this paper.

3.3 Influence of the encapsulating liquid

In this part of the paper we focus our analysis on the influence of the encapsulating phase on the stability limits. For this purpose, we use drops of a glycerol solution at 50% and compare the (X,U) nomograms obtained for collisions with drops of SO M3 and SO M5, see Fig. 13. Note that both pairs of liquids lead to crossing separation. In contrast to the encapsulated phase, the oil phase has a strong influence on the stability limits of the collisions.

Actually, the mean flows generated by the collisions are located in the thin film coming from the encapsulating drop spreading around the aqueous drop. Observing head-on collisions at different relative velocities, we notice that the time needed for the oil to arrive on the other side of the glycerol and generate a closed shell is almost constant when the impact velocity is varied: for $U = 2.23m/s$, t=813μs; for U=2.463m/s, t=806μs; for U=2.60m/s, t=844μs; and for U=2.76m/s, t=833μs. Assuming that the spreading velocity of the oil U_{spread} (in the θ direction of a

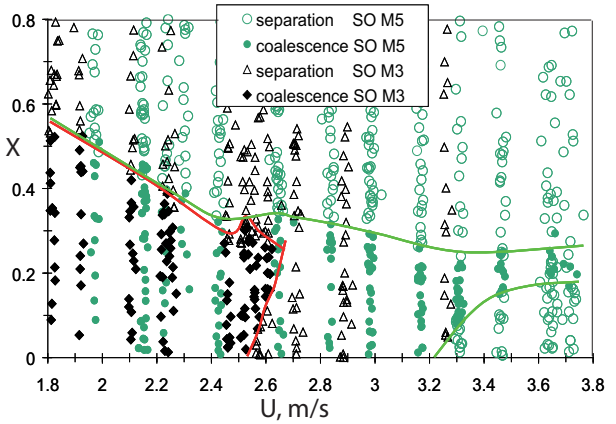

Figure 13: $(X,\ U)$ nomogram for glycerol at 50% with SO M3 and SO M5. The black symbols correspond to G 50% and SO M3. In both cases the drop diameter is 200μm $\pm 10\%$. The oil viscosity changes the head-on stability limits.

spherical coordinate system) is not affected by the relative velocity of the drops, the dissipation associated to this flow is independent of U and can be written as: $E_{visc} \approx \int_t dt \int_{V_o} \mu_o \left(r\partial \left(v_\theta/r\right)/\partial r\right)^2 dV \propto A\mu_o$, where A is a constant, μ_o the oil viscosity, $r\partial \left(v_\theta/r\right)/\partial r \propto U_{spread}/h$, and h is the thickness of the coating layer. This view is in good agreement with the experimental results: U_0 (SO M3)=2.55m/s, U_0 (SO M5)=3.25m/s, which leads to a kinetic energy ratio of 0.61. The viscosity ratio is $2.79/4.57 = 0.611$.

By further increasing the oil viscosity, while keeping the same glycerol concentration, we change the head-on separation mechanism (see Table 2). But if the main dissipation occurs at the early stage of the encapsulation, and if the oil spreading velocity is really constant, the previous description still holds, and the same behavior should be seen for the other oils. To estimate the spreading velocity of the oil, we record the collisions at different instants. This procedure is possible by aliasing the frequency of drop formation and the frequency of illumination, which produces moving pictures of the drops with continuously varying phase. From those movies we extract both the maximum diameter of the merged drop, D_{max}, and the time needed to reach this maximum $t(D_{max})$. The time $t = 0$ is taken at the contact time. It appears (Fig. 14) that the evolution of D_{max} with $t(D_{max})$ is linear and quasi similar for all further investigated oils: SO M10, SO M20, and the two mixtures 1:1 SO M5 + SO M10 and SO M10 + SO M20. Now, looking at the stability limit of the head-on collisions, we plot in Fig. 15 the threshold velocity versus the oil viscosity (the glycerol concentration is kept constant at 50%). Despite the fact that all

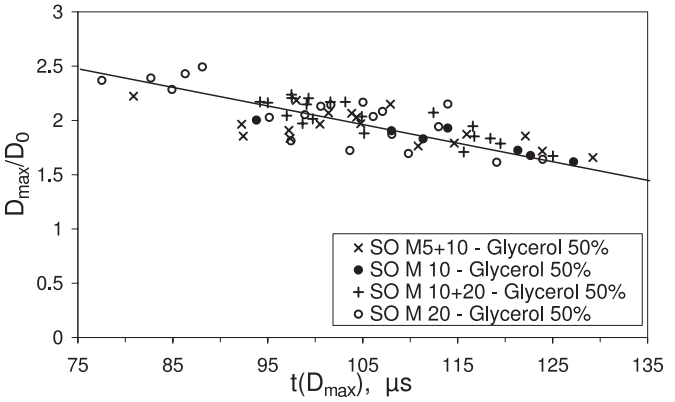

Figure 14: Evolution of D_{max}/D_0 with $t(D_{max})$. Investigated oil phases: SO M5 + SO M10, SO M10, SO M10 + SO M20, and SO M20. 2.3m/s $<$ U $<$ 7.0m/s involving full coalescence and separation. The linear evolution allows us to consider the spreading velocity of the oil constant.

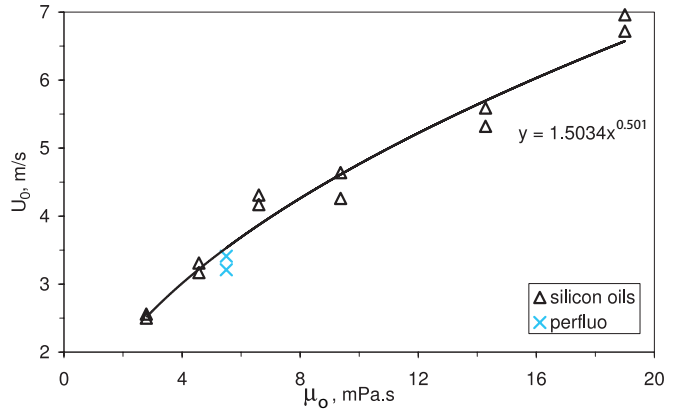

Figure 15: Evolution of the threshold velocity U_0 of head-on collisions with μ_o. The encapsulated phase is G 50%. The data include six silicon oils (SO M3; SO M5; SO M5 + SO M10; SO M10; SO M10 + SO M20 and SO M20) plus the perfluorodecaline. The scaling law $U_0 \propto {\mu_o}^{1/2}$ is in good agreement with the experimental values.

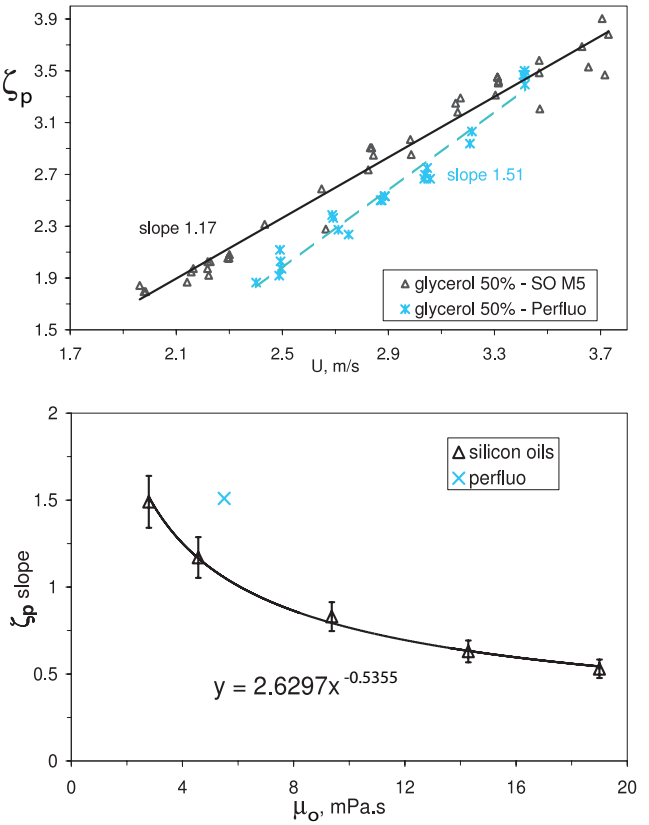

Figure 16: Top: Evolution of ζ_p with U for SO M5/G 50% and for perfluo/G 50%. The drops have a diameter of approximately $200\mu m$. Bottom: growth rate of ζ_p as a function of the oil viscosity.

different mechanisms can be seen for the head-on separation, the agreement with the scaling law $U_0 \propto {\mu_o}^{1/2}$ is very good, see Fig. 15. This evolution of U_0 with μ was already found by Jiang, Umemura, and Law (1992) for drops of equal liquids. To extend our study to the influence of the encapsulating phase, experiments with perfluorodecaline have been carried out. As shown in Table 1, this allows us to vary the oil density, keeping the viscosity and surface/interfacial tensions in the range of the one of SO M5. Here, again, we observe that the stability limit for head-on collisions is well described by $U_0 \propto {\mu_o}^{1/2}$. The difference in momentum prevents a regular distribution of the oil around the glycerol solution. This can be directly seen in Figs. 8 and 9. This two-headed distribution of the oil modifies the growth rate or ζ_p (Fig. 16), but does not strongly change U_0 (Fig. 15).

3.4 Encapsulation efficiency

With the aim to use such binary collisions for liquid encapsulation of one liquid in an immiscible other one, it is important to control the thickness of the shell. In the case of stretching separation, the outcome always consists of the full aqueous drop encapsulated by an oil film and a smaller pure oil drop with some potential satellites, all of pure oil. In contrast to head-on collisions, such a configuration ensures the encapsulation of the full aqueous drop. Measuring the difference between the volumes of the drops of the coated liquid upstream ($V_{w,i}$) and downstream from the impact point($V_{w,f}$), it is possible to calculate the volume $\Delta V_c = V_{w,f} - V_{w,i}$ of the oil forming the shell. Its non-dimensional form is defined as $\varphi = \Delta V_c / V_{o,i}$, where $V_{o,i}$ is the initial oil drop volume (volume of the coating drop upstream from the impact point). In cases of permanent coalescence of the two drops, $\varphi = 1$. We first vary, for a given pair of liquids (SO M3 and Glycerol at 50%), the impact velocity and measure φ (see Fig. 17) for different impact parameters. The amount of oil left around the aqueous core diminishes with increasing X, but does not change with U. Changing the concentration of the glycerol solution or the oil phase (see Fig. 18) shows the same behavior: the only parameter on which φ depends is X. In other words, the thickness of the shell can easily be tuned by changing X without taking into account the relative velocity or the pair of liquids processed. This phenomenon is a big advantage for industrial applications.

Comparing the results of Figs. 18 top and 18 bottom, we see that if we take into account the error bars (not represented in Fig. 18 for clarity), all points collapse on one line. The dashed lines of Figs. 18 top and 18 bottom ("pure geometric capture") assume that the quantity of oil coating the aqueous drop corresponds to the inter-

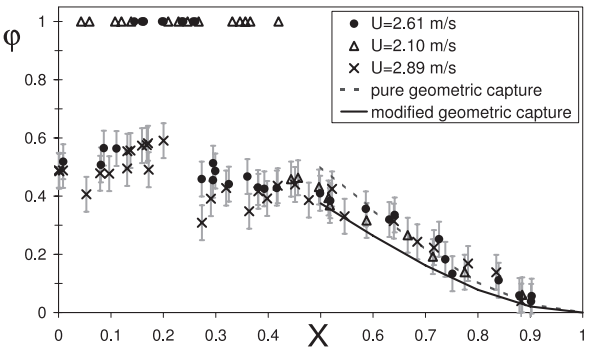

Figure 17: Evolution of φ with X at different impact velocities. Aqueous phase: G 50%; oil phase: SO M3.

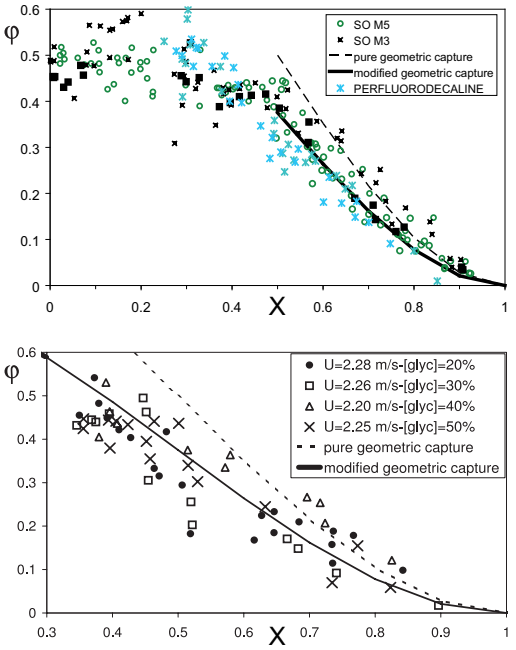

Figure 18: Top: Evolution of φ with X for different oils with aqueous phase G 50%. Bottom: Evolution of φ with X for different glycerol concentrations with oil SO M3.

acting volume of the colliding drops defined in Fig. 19. For $X > 0.5$, the non-dimensional interacting volume can be written as a function of X: $\varphi = (1-X)^2 \cdot (1+2X)$. The experimental volumes, however, are slightly smaller. This may be due to the fact that, while the drops come into contact, they are distorted and may slightly rotate. Considering this possible explanation, our geometrical argument agrees quite well with the experimental data. Taking 75 % of the geometric interaction volume, the resulting curve represents the measured coating volumes very well.

3.5 Unequal-sized drops

The case of unequal-sized drops is briefly touched in this section. Our motivations are to better understand these collisions, but also to generalize the encapsulation application by broadening the stability of full coalescence or by developing the possibility to have a shell volume bigger than the core. Because the generation of our droplets is based on the Rayleigh instability, their production at a given

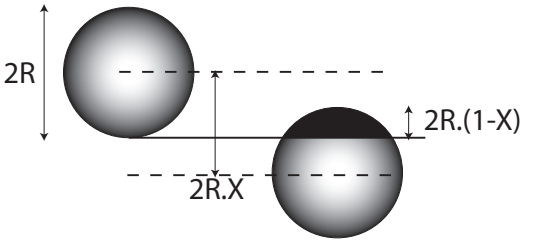

Figure 19: Interacting volume for off-center collisions with $X > 0.5$. Its non dimensional form is $\varphi = (1-X)^2 \cdot (1+2X)$.

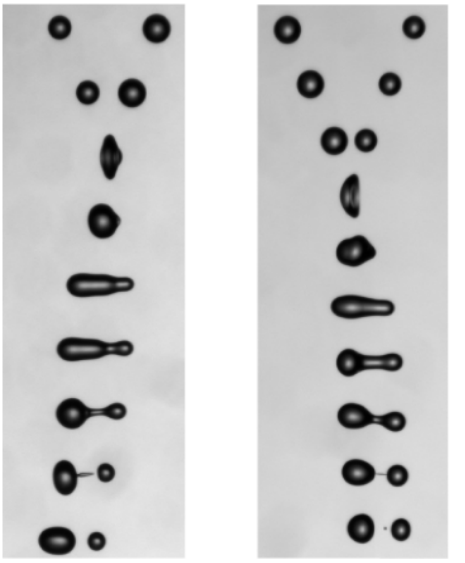

Figure 20: Collisions of G 50% and SO M3 drops. Left: D_o=155μm, D_G=185μm, U=3.43m/s and X=0. Right: D_o=180μm, D_G=150μm, U=3.14m/s and X=0.02. The oil is expelled due to crossing separation.

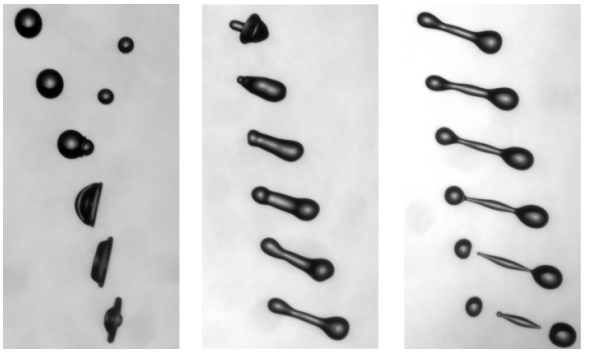

Figure 21: Collisions of G 50% and SO M3 drops. D_o=358μm, D_G=202μm, U=5.23m/s and X=0.05. The oil is expelled due to reflexive separation.

frequency limits their size ratio (Brenn (2000)). For this reason, we worked with the following combinations:

- drops of SO M3 with $D_o \approx$155μm plus drops of a glycerol solution at 50% with $D_G \approx$185μm. This size ratio corresponds for these two liquids to a momentum ratio oil/glycerol (M_o/M_G) of 0.46.
- drops of SO M3 with $D_o \approx$180μm plus drops of a glycerol solution at 50% with $D_G \approx 150\mu$m for $M_o/M_G = 1.37$.
- drops of SO M3 with $D_o \approx$350μm plus drops of a glycerol solution at 50% with $D_G \approx 200\mu$m for $M_o/M_G = 4.24$.

Note that the momentum ratio given by perfluorodecaline / glycerol at 50% with equal sized drops of 200μm diameter (as in Fig. 9) is 1.72.

For $M_o/M_G = 0.46$, i.e. when the oil phase has to spread around an aqueous drop with a higher momentum, we observe that the stability limit for head-on collisions is moved to $3.19 \leq U_0 \leq 3.28 m/s$. In comparison, for equal sized drops (D_o=D_G=195μm $\pm$5%), we have: 2.52m/s $\leq U_0 \leq$ 2.56m/s. A similar stabilization is also seen for $M_o/M_G = 1.37$ with 2.97m/s $\leq U_0 \leq$ 3.14m/s. In both cases, the pictures of the collisions indicate that crossing separation occurs, compare Fig. 20 with Fig. 7. This means that, in the case of an oil drop smaller than the aqueous one (here $M_o/M_G = 0.46$), less oil is available in the excrescence. As a result, more kinetic energy is needed to stretch it until the modified Rayleigh criterion is reached and leads to its break-up. Note that ζ_p is found to be 3.05, which is in very good agreement with the values found for equal sized drops and tends to validate

our point of view on crossing separation break-up. In contrast, when the oil drop is bigger than the aqueous one (here $M_o/M_G = 1.37$), a bigger volume of oil has to flow, leading to higher viscous losses. For this reason, the growth of the excrescence is limited, and the stability is enhanced. The measurement of the critical ζ_p gives a value between 2.85 and 2.95, which corroborates our statement about the limited growth of the excrescence while staying in the range of our modified Rayleigh criterion.

When increasing M_o/M_G further to 4.24, the stability of the head-on collisions is further increased: $4.14 \leq \mathrm{U}_0 \leq 5.22$ m/s. The broad range of U_0 is due to the difficulty to identify the transition with the recorded frames. It is also interesting to point out that the mechanism for the head-on separation is not the crossing separation any more. As for perfluorodecaline, reflexive separation takes place, see Figs. 21 and 9. At the moment we may simply identify that, for a given viscosity ratio of the two liquids, the momentum ratio of the two drops determines the mechanism of the head-on separation. We hope that our ongoing work will bring a good theoretical explanation of this observation.

4 Conclusions

We presented experimental investigations on immiscible liquid droplet collisions for encapsulation. Aqueous glycerol solutions were tested with several silicon oils and one fluorinated oil. We survey the different outcomes of such collisions and compare them to the more classical case of collisions between drops of the same liquid. Even if the regimes are very similar, we show that the processes leading to head-on separation are completely different. For immiscible liquids we identified three mechanisms: crossing separation, single-reflex separation, and reflexive separation. The viscosity ratio plus the momentum ratio control the process of separation. The threshold velocity for head-on separation scales as the square root of the encapsulating liquid viscosity. In the crossing separation domain, this threshold velocity is not modified by changing the encapsulated phase viscosity by a factor 4. For unequal-sized drops, the full encapsulation can be achieved for higher velocities, regardless which drop is the bigger one. Another way to vary the shell thickness is to work with off-center collisions. In the domain where $X > 0.5$, the coating thickness can be tuned by varying the impact parameter, independently of both the pair of liquids and the relative velocity of the drops. As a result, binary collisions of immiscible liquid drops appear as a very promising and reliable way to encapsulate a liquid.

Acknowledgement: We acknowledge financial support from the Hubert Curien Program AMADEUS 2009 from the French Ministry of Foreign Affairs and the

Austrian ÖAD. Financial support from the Steiermärkische Landesregierung for C.P. is gratefully acknowledged. We also acknowledge financial support from the European Cost Action P21 - Physics of Droplets. We wish to thank the institute TVTUT of Graz University of Technology for support in the measurements of interfacial tensions.

References

Ashgriz, N.; Poo, J. (1990): Coalescence and separation in binary collisions of liquid drops. *J. Fluid Mech.*, vol. 221, pp. 183–204.

Brazier-Smith, P.; Jennings, S.; Latham, J. (1972): The interaction of falling water drops: coalescence. *Proc. R. Soc. London A*, vol. 326, pp. 393–408.

Brenn, G. (2000): On the controlled production of sprays with discrete polydisperse drop size spectra. *Chem. Eng. Sci.*, vol. 55, pp. 5437–5444.

Brenn, G.; Tropea, C.; Durst, F. (1996): Monodisperse sprays for various purposes - their production and characteristics. *Part. Part. Syst. Charact.*, vol. 13, pp. 179–185.

Brenn, G.; Valkovska, D.; Danov, K. (2001): The formation of satellite droplets by unstable binary drop collisions. *Phys. Fluids*, vol. 13, pp. 2463–2477.

Chen, R.-H. (2007): Diesel-diesel and diesel-ethanol drop collisions. *Appl. Thermal Eng.*, vol. 27, pp. 604–610.

Chen, R.-H.; Chen, C.-T. (2006): Collisions between immiscible drops with large surface tension difference: diesel oil and water. *Exp. Fluids*, vol. 41, pp. 452–461.

Gao, T.-C.; Chen, R.-H.; Pu, J.-Y.; Lin, T.-H. (2005): Collision between an ethanol drop and a water drop. *Exp. Fluids*, vol. 38, pp. 731–738.

Gotaas, C.; Havelka, P.; Jakobsen, H.; Svendsen, H.; Hase, M.; Roth, N.; Weigand, B. (2007): Effect of viscosity on droplet-droplet collision outcome: experimental study and numerical comparison. *Phys. Fluids*, vol. 19, pp. 102–106.

Jiang, Y.; Umemura, A.; Law, C. (1992): An experimental investigation on the collision behaviour of hydrocarbon droplets. *J. Fluid Mech.*, vol. 234, pp. 171–190.

Orme, M. (1997): Experiments on droplet collisions, bounce, coalescence and disruption. *Prog. Energy Combust. Sci.*, vol. 23, pp. 65–79.

Planchette, C.; Lorenceau, E.; Brenn, G. (2010): Liquid encapsulation by binary collisions of immiscible liquid drops. *Colloids Surf. A: Physicochem. Eng. Aspects*, vol. 365, pp. 89–94.

Qian, J.; Law, C. (1997): Regimes of coalescence and separation in droplet collision. *J. Fluid Mech.*, vol. 331, pp. 59–80.